Visualizing the effect of dynamin inhibition on annular gap vesicle formation and fission

Beth Nickel[1], Marie Boller[1], Kimberly Schneider[1], Teresa Shakespeare[2], Vernon Gay[1] and Sandra A. Murray[1,*]

[1]Department of Cell Biology and Physiology, University of Pittsburgh, School of Medicine, Pittsburgh, PA I5261, USA
[2]Department of Biological Sciences, Fort Valley State University, Fort Valley, GA 31030, USA
*Author for correspondence (smurray@pitt.edu)

Accepted 11 March 2013
Journal of Cell Science 126, 2607–2616

doi: 10.1242/jcs.116269

Summary

Although gap junction plaque assembly has been extensively studied, mechanisms involved in plaque disassembly are not well understood. Disassembly involves an internalization process in which annular gap junction vesicles are formed. These vesicles undergo fission, but the molecular machinery needed for these fissions has not been described. The mechanoenzyme dynamin has been previously demonstrated to play a role in gap junction plaque internalization. To investigate the role of dynamin in annular gap junction vesicle fission, immunocytochemical, time-lapse and transmission electron microscopy were used to analyze SW-13 adrenocortical cells in culture. Dynamin was demonstrated to colocalize with gap junction plaques and vesicles. Dynamin inhibition, by siRNA knockdown or treatment with the dynamin GTPase inhibitor dynasore, increased the number and size of gap junction 'buds' suspended from the gap junction plaques. Buds, in control populations, were frequently released to form annular gap junction vesicles. In dynamin-inhibited populations, the buds were larger and infrequently released and thus fewer annular gap junction vesicles were formed. In addition, the number of annular gap junction vesicle fissions per hour was reduced in the dynamin-inhibited populations. We believe this to be the first report addressing the details of annular gap junction vesicle fissions and demonstrating a role of dynamin in this process. This information is crucial for elucidating the relationship between gap junctions, membrane regulation and cell behavior.

Key words: Gap junction dynamics, Connexins, Annular gap junction vesicle, Fission, Dynamin, Endocytosis

Introduction

Gap junction channels are composed of proteins called connexins (Goodenough et al., 1996). Connexin 43 (Cx43) gap junction protein, the most ubiquitously expressed connexin, is thought to be synthesized in the endoplasmic reticulum, oligomerized into a hemichannel in the Golgi (Ahmad et al., 1999) and then be transported to the cell surface to form the channels that cluster into gap junction plaques (Goodenough et al., 1996). It has been demonstrated by a number of investigators that gap junction plaques are removed from the surface by an internalization, 'endoexocytosis' process that results in the formation of a double-membraned (pentalaminar) vesicle, which has been termed an annular gap junction (Jordan et al., 2001; Larsen and Hai-Nan, 1978; Larsen et al., 1979) or connexosome (Leithe et al., 2006a). It has been suggested that these annular gap junction vesicles may 'fragment' to form smaller vesicles (Piehl et al., 2007). While this fission process has been suggested to facilitate gap junction vesicle degradation (Piehl et al., 2007), the details and molecular mechanism involved in this process are not known.

With quantum dot immuno-electron microscopy, we have confirmed that clathrin is part of the coat surrounding these pentalaminar annular gap junction vesicles (Nickel et al., 2008; Ogunkoya et al., 2009). In addition, at the light microscopic level of resolution, clathrin and its adaptor proteins, adaptor protein 2 (AP-2), epsin and disabled 2 (DAB2), have been shown to colocalize with Cx43 gap junction plaques (Gumpert et al., 2008; Larsen et al., 1979; Ogunkoya et al., 2009; Piehl et al., 2007). These findings are consistent with gap junction plaque internalization being a clathrin-mediated process and it is thought that the formation of a clathrin/adaptor protein/connexin complex results in the invagination of the gap junction plaque membrane.

The internalization of the invaginated gap junction plaque membrane is a critical step in the removal of gap junction plaques from the plasma membrane and thus annular gap junction vesicle formation. It is thought that the frequency of gap junction plaque internalization and subsequent annular gap junction vesicle degradation may impact a number of pathological conditions, including cancer and ischemia (Fiorini et al., 2008; Leithe et al., 2006b; Murray et al., 1981), and further may also be critical to numerous cellular functions, such as cell migration, proliferation, and wound healing (Chanson et al., 2005; Defranco et al., 2008).

Dynamin, a molecule that has been well documented to facilitate endocytosis of other types of vesicles from the membrane (De Camilli et al., 1995; Hill et al., 2001; Iversen et al., 2003; Kirchhausen, 2000a; Kirchhausen, 2000b; Kirchhausen et al., 2008; Rappoport et al., 2008; Roux and Antonny, 2008), has been previously shown to colocalize with gap junction plaques and annular gap junction vesicles in cells expressing Cx43-GFP protein (Gumpert et al., 2008). Based on this initial finding, it was suggested that dynamin facilitates the formation and release of gap junction buds from the membrane to form annular gap junction vesicles, similar to its scissoring function in the release of other membrane vesicles (Hill et al., 2001; Kirchhausen et al., 2008). During the internalization of

Journal of Cell Science

membrane vesicles it has been demonstrated that dynamin forms a lattice that then constricts to pinch the buds from the membrane (Hill et al., 2001; Kirchhausen et al., 2008). Certainly, the possibility of such a fission process during gap junction plaque internalization and annular gap junction formation is supported not only by the immunocytochemical colocalization studies (Piehl et al., 2007), but also by studies in which inhibition or reduction of dynamin activity (by expression of the dominant negative dynamin, or treatment with dynasore or GTPase gamma) in cells transfected to express fluorescently tagged Cx43 gap junction protein (Cx43-GFP), resulted in significantly fewer annular profiles (Gilleron et al., 2011; Gumpert et al., 2008).

Dynamin has been suggested to act at two steps during the formation of other (non-gap junctional) clathrin coated vesicles, namely, recruiting clathrin to the invaginating membrane (and thus the formation of a U-shaped structure) and fission of the pit from the membrane (Kirchhausen et al., 2008; Macia et al., 2006; Nankoe and Sever, 2006). Here we suggest in addition that dynamin acts in the cytoplasm to constrict the annular gap junction vesicle and facilitate vesicle fission. Unlike the fission events that have been previously described to occur at the cell surface that result in formation of a single-membraned vesicle, gap junction plaque membrane internalization results in the formation of double-membraned annular gap junction vesicle. In addition, the size of an annular gap junction vesicle is a relatively large structure compared to the thin stalk area of a single membraned bud, thus posing additional challenges in understanding the annular gap junction fission process.

In this study, the morphological changes in gap junction plaques and annular gap junction vesicles in living cells were imaged in the presence or absence of treatments that inhibit dynamin activity. From our findings, we demonstrate that cells are capable of forming bud-like projections from the gap junction plaque in control and dynamin inhibited populations. However, in the presence of the dynamin inhibitor (dynasore) or in siRNA dynamin knockdown cells, the majority of these buds fail to be released from the plasma membrane, in contrast to the relatively rapid release of these structures from plaques in the control populations. Moreover, we have demonstrated, to our knowledge for the first time, that annular gap junction vesicle fission was decreased when dynamin was inhibited and we thus suggest a unique role for dynamin in annular gap junction vesicle processing.

Results

Dynamin association with gap junction plaques and annular vesicles

Given the known role of dynamin in the scissoring of other endocytic vesicles from the membrane, and the report that dynamin colocalizes with gap junctions in cells transfected to express fluorescently tagged Cx43, we investigated first the association of dynamin with gap junction structures and annular gap junction formation in cells that endogenously expressed Cx43. In these cells, both clathrin and dynamin were demonstrated to colocalize with gap junction plaques (Figs 1, 2), and dynamin was found particularly at areas where the plaques were invaginated or appeared to be forming buds (Fig. 2C,D). In addition dynamin associated with some of the cytoplasmic puncta, which based on their size are thought to represent annular gap junction vesicles, rather than other structures such as secretory vesicles containing newly synthesized Cx43. Secretory vesicles have been demonstrated to be less than 0.150 μm (Evans and Martin, 2002) while annular gap junction vesicles are much larger (≥0.5 μm) (Jordan et al., 1999). Dynamin colocalized with 26.2±2.5% of the structures identified as annular gap junction vesicles while 25.8±4.4% of the gap junctions plaques were associated with dynamin. Furthermore, by rotating the axis of cell populations co-stained to localize Cx43 gap junction protein and dynamin, we found that dynamin associated mainly with a central, equatorial, region of the annular gap junction vesicle surface but did not coat the entire

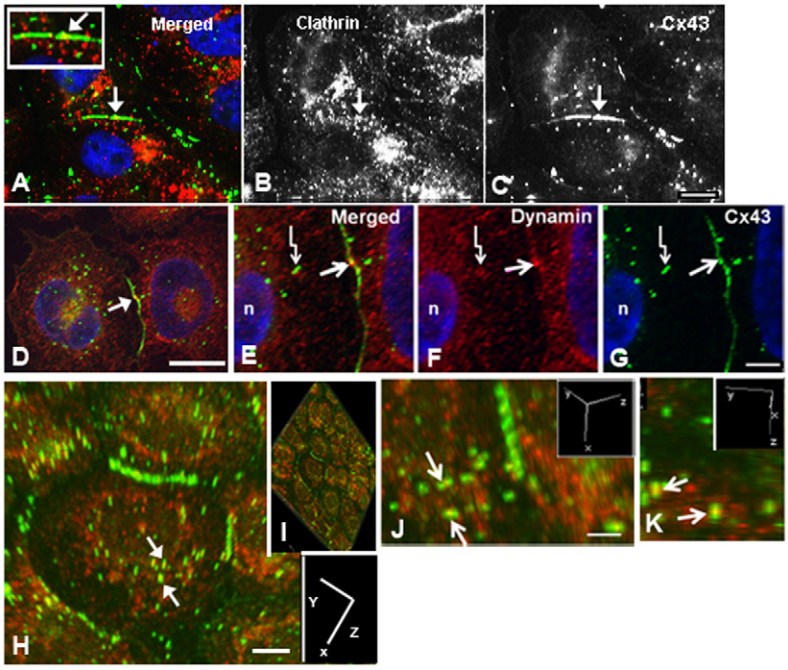

Fig. 1. Immunocytochemical colocalization of the Cx43 protein with clathrin or dynamin in human adrenal tumor cells. (**A–K**) Colocalization of Cx43 protein (C and green in A) with clathrin (B and red in A) or dynamin (red in D–K) is shown. Note the colocalization (yellow) in the merged images with clathrin (A) and dynamin (D,E,H–K) in an area of the gap junction plaque (arrows in A–G) and annular gap junction vesicles (crooked arrows in E–G). Confocal microscopy techniques coupled with image rotation (a function within Nikon Elements that allowed us to reconstruct 3D images) shows the colocalization of dynamin at or near the equator of the annular gap junction vesicles (arrows in H,J,K). The axis of rotation is shown in the inserts in H–K. Scale bars: 10 μm (A–C,E–H); 4 μm (D); 5 μm (J,K).

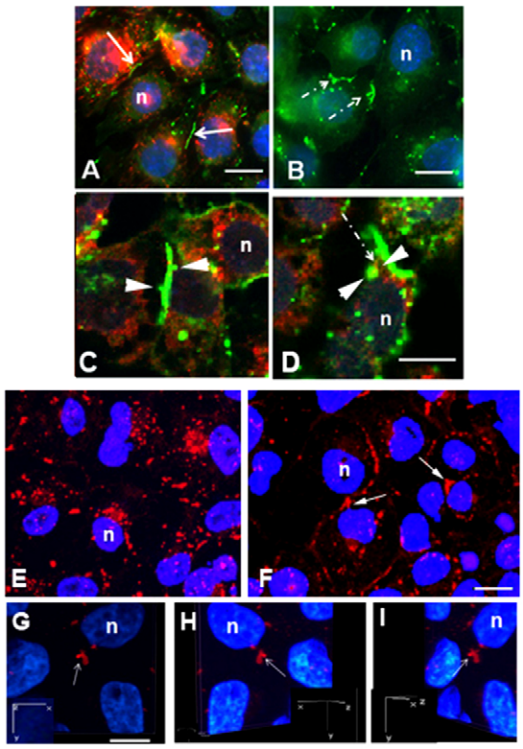

Fig. 2. Immunocytochemical localization of Cx43 gap junction protein in control and dynasore-treated cells. (**A–E**) Cells were treated with 80 μM dynasore (B,D) or diluent (A,C,E) for 1 hour. Transferrin (red) uptake (A,B) was minimal in cells treated with dynasore (B) compared with that seen in controls (A). Note the colocalization (yellow) of dynamin (red in C,D) and Cx43 (green) in an area of the gap junction buds (arrowheads). Typical linear gap junction plaques, some of which had small buds, were evident in control populations (A), whereas gap junction plaques with relatively large gap junction buds (dashed arrows) were prevalent in dynasore-treated cell populations (B). (**F–I**) In the siRNA dynamin knockdown cell populations, there was decrease in the number of annular gap junctions and an increase in the number of gap junction buds (arrows) in cells compared with control populations (E). The attachment of a gap junction bud was demonstrated with confocal immunocytochemical 3D-reconstruction in siRNA knockdown cells (G–I). Inserts represent the rotation around the *y*-axis; n, nucleus. Scale bars: 7 μm (A,B); 10 μm (C,D,G–I); 20 μm (E,F).

vesicle (Fig. 1I–L). This is a location that would be ideally suited to constrict the annular gap junction vesicle and thus facilitate fission.

Immunocytochemical analysis of dynamin inhibition

To determine if dynamin is involved in annular gap junction vesicle formation and fission, cells were treated for 1 hour with 80 μM dynasore, a compound well known to inhibit dynamin GTPase activity (Kirchhausen et al., 2008), or dynamin was knocked down with siRNA techniques. The cells appeared to be healthy and to retain their capacity to proliferate (data not shown). To confirm that dynasore treatment was capable, at the concentration being used and in this cell line, of inhibiting endocytosis, transferrin uptake was measured. Dynasore in this study was demonstrated to inhibit constitutive transferrin endocytosis (Fig. 2A,B). As can be seen in Fig. 2, transferrin which is constitutively taken up by the control cell can be seen within the cytoplasm. It is not seen to accumulate at the cell membrane since it is constitutively taken up by the cell membrane. The cells were not acid-stripped, and the transferrin was allowed to remain on the cells throughout the incubation period as a result, recycling was not detected in the control. In the dynasore-treated population very little transferrin uptake is seen (Fig. 2B).

In the dynasore-treated populations, the frequency of projections from the gap junction plaque, ‘gap junction buds,’ appeared to be increased (Fig. 2B). In contrast, in DMSO control cell populations, only an occasional bud was observed to be attached to gap junction plaques in the immunocytochemical preparations (Fig. 2A,C). Dynamin was demonstrated to associate with the neck region of some of these large gap junction buds (Fig. 2D). It was noted that the buds in dynasore-treated cells appeared larger than those in the control. Consistent with the large and irregular shaped buds seen in immunocytochemical preparations, in the transmission electron microscopic images of dynasore-treated cells, large U-shaped gap junction plaques and gap junction buds were evident (Fig. 3).

Similar to the treatment with dynasore, when dynamin was knocked down, with siRNA knockdown techniques, large bud-like projections from gap junction plaques were also observed (Fig. 2E–I). The use of 3D confocal reconstruction techniques as well as observations made with transmission electron microscopy allowed us to confirm that some of these bud-like structures seen

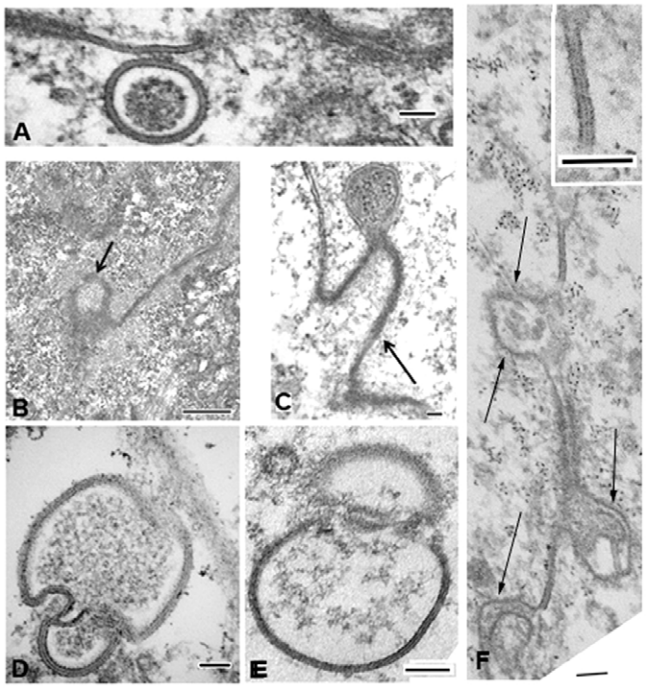

Fig. 3. Gap junction plaques and annular gap junction vesicles in control and dynasore-treated cells. (**A–F**) Transmission electron microscopy images of gap junction plaques and annular gap junction vesicles in control (A,D,E) and dynasore-treated (B–F) populations. Note the annular gap junction vesicle near a gap junction plaque membrane in the control population (A). In the dynasore-treated populations, the invaginated gap junction plaque membrane is evident (arrows in B,C). Annular gap junctions can be seen in control populations which appear to be undergoing fission (D,E). (F) An image of the gap junction plaque in a dynasore-treated cell demonstrates numerous sites of apparent invagination (arrows). The typical gap junction membrane at sites that are not invaginated can be seen. Scale bars: 100 nm (A,C–F); 500 nm (B).

in dynasore-treated and siRNA dynamin knockdown populations were indeed tethered to the surface, and thus true buds, and not annular gap junctions that remained near the plaques (Fig. 2G–I).

To better assess the changes observed in dynamin inhibited populations, the number of buds/plaque was quantitated by the computer-assisted analysis with MetaMorph software. While neither the number nor the size of the gap junction plaques were altered in siRNA dynamin knockdown or in dynasore-treated cultures (data not shown), there were, however, significantly fewer buds/plaque in the control cell populations (0.01 ± 0.01; $n=110$ plaques) than that measured in populations in which dynamin was knocked down (0.16 ± 0.03; $n=112$ plaques).

If the increased number of buds/plaque, in the siRNA dynamin knockdown populations, reflects a decreased capacity for bud release, then a decrease in annular gap junctions would be predicted. We therefore counted and compared the number of annular gap junctions in immunocytochemical images of control and dynamin inhibited or siRNA dynamin knockdown populations. As predicted, when dynamin was knockdown, the average number of annular gap junctions/cell detected was significantly reduced (2.02 ± 0.74; $n=122$ cells) compared to control populations (7.09 ± 0.62; $n=124$ cells).

The measured increase in the number of gap junction buds per plaque, and decrease in annular gap junction vesicles, in dynamin inhibited populations, is consistent with dynamin serving to scissor the gap junction buds from the plasma membrane and form annular gap junctions. However, while immunocytochemical analysis allowed us to demonstrate gap junction plaques with increased numbers of buds, such snapshots did not permit us to determine the origin and, more important, the fate of the gap junction buds and annular gap junction vesicles in these cell populations. Furthermore, this technique did not allow us to determine if the measured decrease in number of annular gap junction vesicles was only a result of failure of the buds to be pinched from the membrane. Therefore, to elucidate the role of dynamin in the dynamic behavior of the gap junction plaques and annular gap junction vesicles, time-lapse imaging was used in cells transfected to express Cx43-GFP.

Live-cell analysis of dynamin inhibition

A detailed examination of the spatial and temporal-dependent distribution of Cx43-GFP revealed gap junction plaque internalization that occurred in two ways; either large segments or the entire gap junction plaque was internalized or smaller punctate-like structures were released from the existing gap junction plaque (Fig 4A,B; supplementary material Movies 1–3). Both processes resulted in the formation of a cytoplasmic annular gap junction vesicle, however, as expected, in a variety of different sizes. Large plaques were seen to first invaginate at or near the central area until they became deeply curved into an U-shaped structure (Fig. 4B2). The U-shaped structure subsequently became bud shaped, with only a thin neck still attaching it to the plaque (Fig. 4B4). The bud, with time, detached from the membrane to form the fully developed annular gap junction vesicle (Fig. 4A4,B6; Fig. 5A,C). Internalization of the smaller buds occurred near the central region of the gap junction plaque (Fig. 5A,C).

In dynasore-treated populations, gap junction buds were observed during the process of formation. The size (area) as well as morphological changes in the buds were monitored over time with the NIS-Elements program (Nikon Instruments Inc., Melville, NY) and the maximum area of a bud during the viewing period was recorded and the maximum areas were averaged. The average size (area) of gap junction buds measured in dynasore-treated cells (2.38 ± 0.23 μm^2; $n=189$ buds) was larger than that measured in DMSO control cell populations (1.40 ± 0.06 μm^2; $n=55$ buds). In addition to the gap junction buds in the dynasore-treated cultures being larger, they remained tethered to the surface, in most cases, for most of the viewing period (Fig. 5B). This is in contrast to the frequent release of the smaller buds detected in the control population (Fig. 5A; supplementary material Movie 2). Some of the gap junction buds elongated in

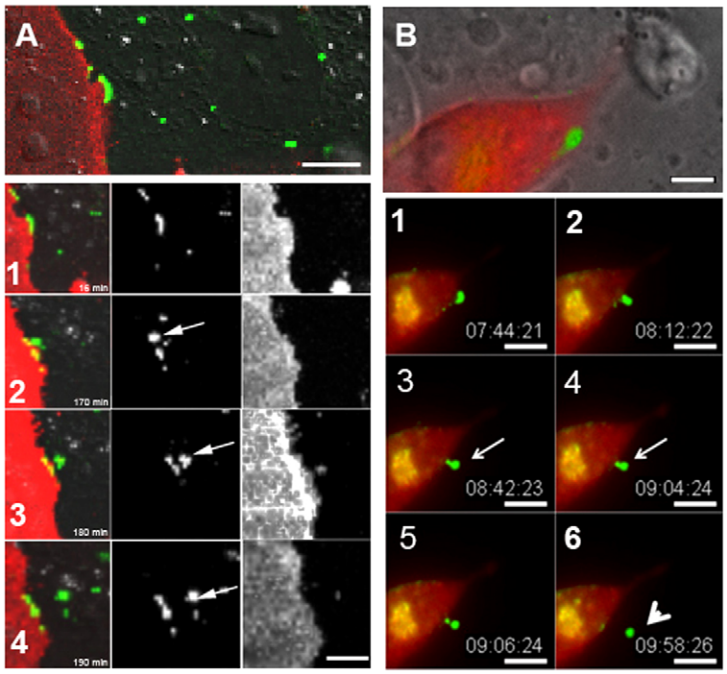

Fig. 4. Time-lapse imaging montage of gap junction plaque endoexocytosis. (**A**,**B**) Upper DIC images show gap junction plaques at time zero. Numbered images below show the gap junctions at the times indicated. Note the internalization of the gap junction plaque (Cx43-GFP) into a cell that is not labeled with the membrane marker, RFP-tagged pCS2 (A) or not expressing the clathrin-mCherry (B). The presence of tagged pCS2 (A) or clathrin (B) in one of the two contacting cells and the absence of that marker in the other cell, as well as the DIC images (A,B) allow delineation of the cell borders. Note that the gap junction plaque in A (arrow in A2) is internalized to form an annular gap junction (arrow in A4) and that a small amount of the cell marker is seen within the annular gap junction vesicle. The gap junction plaque seen in B presumably had already started to invaginate at the time it was selected for time-lapse imaging. The gap junction plaques in B can be seen to invaginate to form a U-shaped projection (B2), which becomes constricted at the neck to result in a bud (arrows in B3,B4) that then is released to form an annular gap junction vesicle (arrowhead) (B6). See supplementary material Movie 1. Scale bars: 10 μm (A,B).

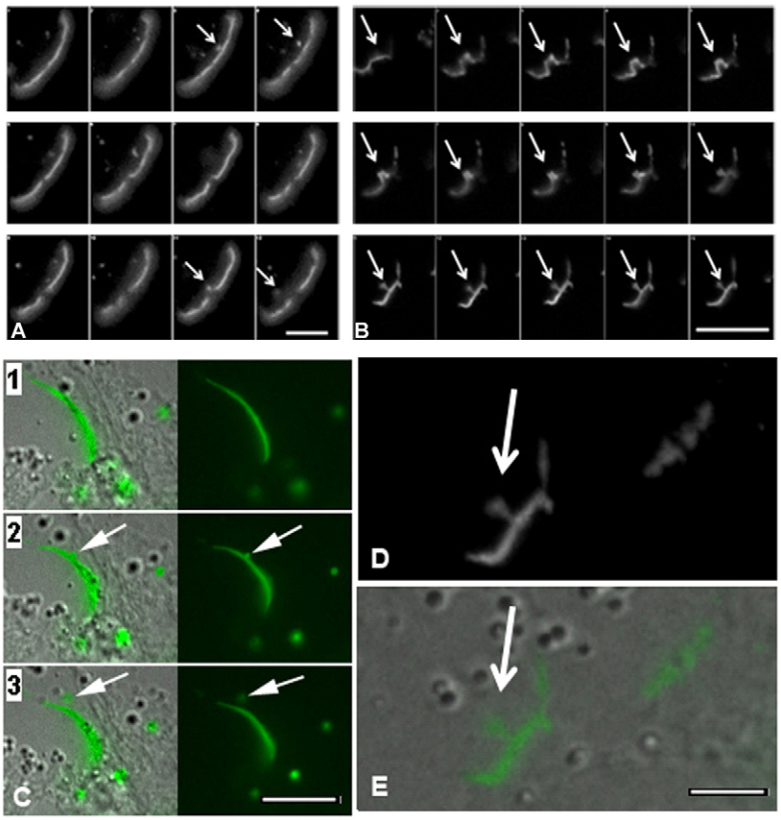

Fig. 5. Time-lapse imaging montage of gap junction plaque endoexocytosis in cells transfected to express Cx43-GFP. (**A**,**C**) Note the relatively rapid formation and release of gap junction buds from the plaque in the control population (arrows). (**B**,**D**,**E**) In cells treated with dynasore, the gap junction bud (arrows) formed and then remained tethered to the gap junction plaque for the duration of the imaging period (7 hours). Corresponding fluorescence and DIC images demonstrate budding (C,E). The bud in B is enlarged in D. See supplementary material Movies 2 and 3. Scale bars: 2.50 μm (A); 5 μm (B); 3 μm (C); 2 μm (D,E).

the dynasore-treated populations and were observed to remain elongated and with a bulb at its tip throughout the viewing period (Fig. 5B; supplementary material Movie 3). Such structures were also observed with immunocytochemical techniques. In the few cases in which gap junction buds were observed to be released, the average area of annular gap junction vesicles formed in the dynasore-treated populations, were significantly larger (0.97 ± 0.09 μm^2; $n=2$) than the average size of annular vesicles formed in the DMSO controls (0.53 ± 0.04 μm^2; $n=20$). Fewer annular gap junction vesicles formed over the 7-hour viewing period in dynasore-treated cultures (13.0 ± 11.8) compared to the number formed over that time in control cell populations (24.0 ± 3.4). The effects of dynasore on gap junction budding were reversible in that when dynasore was washed from the media and the cells were returned to growth media, buds which were tethered to the gap junction plaque were released into the cytoplasm (Fig. 6; supplementary material Movie 4).

We monitored annular gap junction vesicles in control and dynasore-treated populations and visualized fission events by tracking the movement, morphological changes, and the size of individual annular gap junction vesicles over time with the Imaris

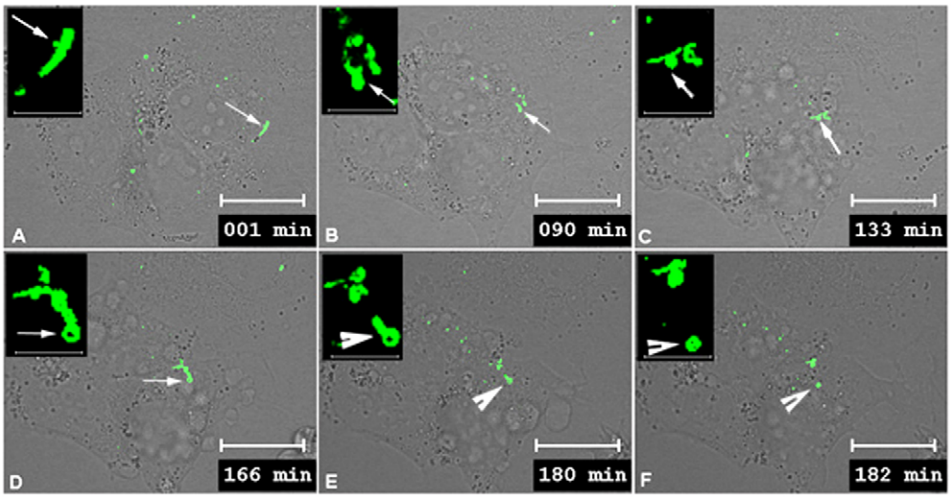

Fig. 6. Montage time-lapse images demonstrating the recovery from dynasore inhibition of internalization. (**A–F**) The cells were imaged for 30 minutes prior to dynasore treatment and then treated for 1 hour with dynasore. For the analysis of recovery, dynasore was washed out. Prior to dynasore treatment, a linear gap junction plaque with a small bud attached was selected for collecting images (arrow) (A). Multiple large gap junction bud-like structures were observed protruding from the gap junction plaque during dynasore treatment (arrows) (B). Once dynasore was washed out and replaced with growth media, one of the buds that could be tethered to the gap junction plaque (C) was seen to internalize and form an annular gap junction (arrowhead) (E,F). See supplementary material Movie 4. Scale bars: 20 μm (A–F); 5 μm (insets).

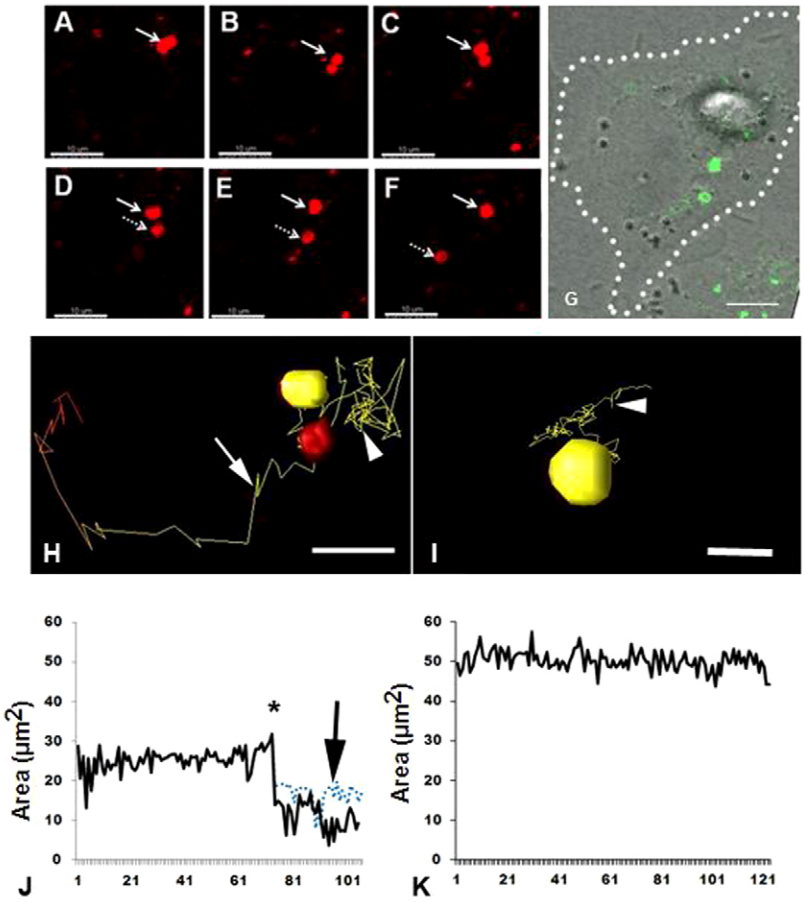

Fig. 7. Monitoring of annular gap junction vesicles and visualization of fission events. (**A–F**) Time-lapse imaging montage of annular gap junction vesicle splitting. (**G**) Corresponding Cx43-GFP/DIC overlay image of E in which the cell border has been delineated by the dotted line. Note the fission of an annular gap junction vesicle in a control cell, which results in the formation of two smaller annular gap junction vesicles. (**H**,**I**) The track taken by the annular gap junction vesicles were followed in control (H) and dynasore-treated cells (I). In H, the annular gap junction vesicle has already split into two smaller annular gap junctions in the control cell. Once the split occurred, one of the vesicles (yellow) continued to move in a Brownian-type pattern (arrowhead), while the second vesicle (red) took a more directional path (arrow). In I, the annular vesicle did not undergo fission and moved in a Brownian-type pattern (arrowhead). (**J**,**K**) Corresponding graphical representations of annular gap junction vesicle size. Vesicle size (area, μm^2) was monitored over time and the control cell (J) decreased at the time corresponding to vesicle fission (asterisk). The size of annular vesicles before and after fission (blue dotted line and black solid line, respectively) is demonstrated. In the dynasore-treated cell (K), the annular vesicle remained constant in size. See supplementary material Movies 5 and 6. Scale bars: 10 μm (A–G); 5 μm (H,I).

analysis software (Bitplane Scientific, South Windsor, CT) (Fig. 7). As seen in the example shown in Fig. 7, a decrease in the area of the annular gap junction vesicle was noted at the point at which fission occurred (arrow in Fig. 7J). Before the fission event, the annular gap junction could be seen to move in a Brownian-like motion (supplementary material Movie 5). In the reconstruction, seen in Fig. 7, the two smaller annular gap junction vesicles, that resulted from the split, moved away from one another. One of the two took a directional path (indicated by the trace line in Fig. 7H, arrowhead) while the second vesicle continued to move in a Brownian-like pattern (indicated by the trace line in Fig. 7H, arrow). Consistent with the observations made with time-lapse imaging techniques, annular gap junction vesicles were revealed with transmission electron microscopic techniques that appeared to be in the process of undergoing fission (Fig. 3D,E).

Given our immunocytochemical observations in which dynamin was found surrounding annular gap junction vesicles at or near their equator (Fig. 1K,L), we used time-lapse imaging techniques to investigate the effect of dynamin inhibition on annular gap junction vesicle fission. The average number of annular gap junction vesicles per hour seen to undergo fission was dramatically reduced in dynasore-treated cultures (0.03 ± 0.02; viewing time=6 hours), compared to the number quantitated in control populations (0.25 ± 0.06; viewing time=3 hours). In addition to vesicle fission, small bud-like projections were seen to project from the surface of the annular gap junction vesicle surface (data not shown). It could not be determined if these structures were being released or if the orientation of the annular vesicle was changing and thus giving an illusion of vesicle release. We did not therefore attempt to quantify these events. When annular gap junctions were tracked in dynasore-treated populations with the Imaris software, unlike in the DMSO control populations (Fig. 7K), there was no significant reduction in the size of the vesicle (Fig. 7I), as would have been expected if the annular vesicle underwent fission. In the dynasore-treated population shown in Fig. 7, the orientation and cellular position of the annular vesicles varied over time as indicated by the trace line (Fig. 7I; supplementary material Movie 6). Based on immunocytochemical localization of dynamin at or near the equator of the annular gap junction vesicle, and the decreased number of fission events in the dynasore-treated populations, we would suggest that dynamin plays a role in the annular gap junction vesicle fission process.

Discussion

In this study we focused on annular gap junction vesicle formation with particular attention on annular gap junction vesicle fission. By obtaining multiple images and generating three-dimensional images that could be rotated, gap junction plaques were viewed from different perspectives and their morphology critically analyzed. We have documented the presence of gap junction buds projecting from the gap junction plaque and have provided evidence, with time lapse imaging, that these buds are formed and released from the gap junction plaques. This is consistent with previous reports describing gap

junction vesicle release mainly from the interior of gap junction plaques (Jordan et al., 1999; Lauf et al., 2002; Segretain and Falk, 2004; Sosinsky et al., 2003). In addition, the internalization of the entire gap junction plaques which we described here is consistent with the light and electron microscopic reports of the relatively large annular gap junction vesicles in this cell line (Larsen et al., 1979; Murray et al., 1997; Ogunkoya et al., 2009).

We have demonstrated that an increase in the number of gap junction buds occurred when dynamin was inhibited by either siRNA knockdown procedures or treatment with dynasore. Our time-lapse images allowed us to conclude that the increased number of buds seen with the immunocytochemical imaging techniques represent a decrease or a failure of the gap junction bud to scissor from the plasma membrane. We thus have provided evidence that dynamin is essential for scissoring of gap junction buds from the plaque and annular gap junction vesicle formation.

Dynamin has been well documented to serve in the scissoring of numerous other types of non-junctional vesicles from membrane (Ungewickell and Hinrichsen, 2007). Specifically, dynamin has been shown to form a spiral around the neck of invaginated membrane during clathrin coated-pit formation. Dynamin would then tighten to constrict and eventually scissor the invaginated membrane from the surface (De Camilli et al., 1995; Hill et al., 2001; Iversen et al., 2003; Rappoport et al., 2008; Robinson, 1994; Roux and Antonny, 2008). Dynamin has been suggested to participate in at least two distinct stages of the formation of other types of vesicles, namely at the scissoring stages and at an early stage during the curvature of the membrane to form the pit or bud (Kirchhausen et al., 2008; Macia et al., 2006; Nankoe and Sever, 2006). This proposed role for dynamin action is based on the reports of coated pit intermediates with either a complete bud-like shape (not yet pinched off) or U-shaped (not yet a fully formed bud) in dynamin inhibited cells (Kirchhausen et al., 2008). Analysis of the morphological changes in gap junction plaque intermediates following dynasore treatment revealed that gap junction plaque segments invaginated to become U-shaped and then went on to form a full bud which remained attached to the plasma membrane by a thin neck. This finding is consistent with dynamin acting only at the step needed to pinch the vesicle from the membrane but not the steps involved in the late stages of invagination.

In earlier studies, dynamin was demonstrated to associate with Cx43-GFP gap junction plaques in cell populations (Gumpert et al., 2008). In this study we have demonstrated this association in cells expressing both native Cx43 and Cx43-GFP. Based on this colocalization data and our time lapse findings, we would suggest that dynamin scissors the gap junction bud from the plasma membrane in a similar manner as that described for other types of vesicles. However one important distinction is that in the case of the gap junction bud there would be a need to scissor a double membrane since the internalization of the gap junction plaque involves the endocytosis of the plasma membrane of the ‘host’ cell as well as the exocytosis of the donor cell.

Fission of the annular gap junction vesicle poses even a greater topological challenge in that it also has a double membrane but unlike the thin neck of the bud, it has a larger area that must be constricted to achieve vesicle fission. It should be noted that these are similar to the challenge faced by mitochondria, in that mitochondria can be similar in size to the annular gap junction vesicles, and they, like the gap junction structures, are double membrane-bound organelles. Mitochondria frequently divide and the molecular machinery involved in mitochondrial fissions has been well established (Elgass et al., 2013; Hoppins et al., 2007; Scott and Youle, 2010). During mitochondrial fissions two members of the dynamin superfamily, dynamin-related proteins (Dnm1) in yeast, and dynamin-related protein (DRP 1) in mammals, assemble into punctate structures on mitochondria surfaces. It is thought that these molecules facilitate the constriction and subsequent scissoring of the mitochondria into two smaller mitochondria (Hoppins et al., 2007; Smirnova et al., 2001; Strack and Cribbs, 2012). A similar process is suggested for the annular gap junction vesicle fission process. Annular gap junction vesicles have been previously reported to fragment (Piehl et al., 2007). This fragmentation process has been described as being similar to vesicle budding, in that the sizes of the fragments were generally small. Although in both DMSO and dynasore-treated populations, we saw similar small buds that protruded from the surface of the annular gap junction vesicle, we were unable to confirm that these small projections were actually released from the bud rather than that the annular gap junction vesicle rotated in such a plane as to give the illusion of bud release.

We, as well as others (Gumpert et al., 2008), have documented a decrease in the number of annular gap junction vesicles in dynasore-treated populations. This decrease has been suggested to reflect the reduction in annular gap junction vesicle formation in dynasore-treated populations. However, based on our observations of a decrease in annular gap junction fission when dynamin was inhibited, we now suggest that such a finding could also be explained by a decrease in annular gap junction vesicle fission. In addition, the possibility that a change occurs in the half-life of the annular gap junction vesicle once internalized has not been ruled out. We suggest a change in annular gap junction vesicle number reported in many studies could result from other processes in addition to gap junction internalization.

It is noted that dynasore is a cell-permeable inhibitor of the GTPase activity of dynamin1, dynamin2 and dynamin-related protein (Drp1) (Kirchhausen et al., 2008; Macia et al., 2006). Dynasore treatment could therefore impact a number of mechanisms and events in addition to those involving gap junctions. However, the increase in gap junction buds in both dynasore-treated and siRNA dynamin knockdown populations, strengthens the argument that dynamin plays a critical role in annular gap junction vesicle formation and that dynasore is a valuable pharmacological tool for the study of dynamin inhibition. The number of annular gap junctions was significantly larger in the siRNA knockdown populations compared to controls while the difference in number of annular gap junction vesicles in dynasore-treated compared to controls did not reach levels of significance. Differences observed in effects of the two methods used to inhibit dynamin may reflect the longer time of dynamin inhibition in the siRNA knockdown populations (24 hours) compared to that of dynasore-treated populations (1 hour).

That the cells can recover following washing out dynasore would suggest that dynasore is acting as a specific inhibitor of dynamin rather than as cellular toxin. Furthermore, that the effect of dynasore can be reversed is consistent with the findings of others who have demonstrated that the inhibitory effects on cell migration (Macia et al., 2006) and on cystic fibrosis transmembrane conductance regulator (CFTR) uptake (Young

et al., 2009) could be reversed when dynasore was washed from the media. In addition, transferrin uptake, which is widely used for the analysis of receptor-mediated endocytosis (Bachran et al., 2011; Sigismund et al., 2005), was inhibited in our study by dynasore treatment. The decrease in transferrin uptake, in the dynasore-treated populations, serves to demonstrate the ability of dynasore to inhibit receptor-mediated endocytosis in this cell line. The data presented here confirms and extends the description of the process by which the gap junction plaque is internalized from the surface to the cytoplasm of the adrenal cell to form an annular gap junction vesicle and is consistent with a role of dynamin in the scissoring needed to release annular gap junction vesicles into the cytoplasm. We report to our knowledge for the first time, the details of annular gap junction vesicle fission. Such fissions may be critical to gap junction protein degradation but the cellular need for this process can at this point, only be speculated and remains to be elucidated. Both lysosomal and more recently autophagolysosomal degradation of the annular gap junction vesicle have been demonstrated (Bejarano et al., 2012; Fong et al., 2012; Lichtenstein et al., 2011; Murray et al., 1981). In addition, other mechanisms of internalization may exist for removing gap junction proteins from the cell surface that do not result in annular vesicle formation, possibly involving lipid rafts (Kirkham and Parton, 2005), and caveolin (Kirkham and Parton, 2005). In addition to degradation, the fission process could, potentially participate in the Cx43 recycling back to the plasma membrane. Gilleron and colleagues, for example, have suggested based on the association of annular gap junctions with two Rab family members of small GTPases known to be involved in recycling, Rab 4 and Rab 11, that annular gap junction budding may facilitate the return of Cx43 to the cell membrane (Gilleron et al., 2011).

It is thought that a multitude of molecular factors are needed to coordinate both gap junction plaque disassembly and gap junction protein turnover. For example, a number of kinases [including protein kinase C (PKC), mitogen-activated protein kinase (MAPK), Casein kinase 1, and pp60^{src} kinase (Src)] have been demonstrated to influence gap junction plaque internalization (Solan and Lampe, 2009). It has been demonstrated that protein kinase activation can results in the phosphorylation of at least 12 serine and 2 tyrosine sites in the C-terminus of Cx43. It is thought that this in turn affects plaque assembly, gating, and internalization (Pahujaa et al., 2007; Solan and Lampe, 2005; Solan and Lampe, 2009). How kinase activation might facilitate the recruitment and/or binding of the endocytic machinery, including dynamin, that is needed for gap junction plaque endocytosis has not been elucidated. It has been reported however that Src kinase phosphorylates clathrin which then promotes redistribution clathrin to the cell membrane and the internalization of epidermal growth factor internalization. Consistent with this, Src promotes the recruitment of the clathrin adaptor protein, AP-2, to beta-arrestin and the angiotensin II type 1 receptor during clathrin-mediated internalization of angiotensin II (Fessart et al., 2005). In those studies, stimulation of the angiotensin II receptors resulted in the formation of an endogenous complex containing Src, beta-arrestin, and AP-2 (Fessart et al., 2005) and the recruitment of clathrin to this complex. It is possible that a similar process exist in which a Src-Cx43–AP-2–dynamin complex forms as part of the regulating machinery for gap junction internalization and subsequent annular gap junction fissions. We speculate that phosphorylation of specific sites on the C-terminal tail of Cx43 facilitates gap junction internalization and annular vesicle fission. Future studies designed to increase our understanding of gap junction plaque internalization and the molecules involved are critical to our knowledge of cell-cell communication in general and may prove to be key for the development of therapies to affect cellular behavior.

Materials and Methods

Cell culture

SW-13 human adrenocortical tumor cells (American Type Culture Collection, Rockville, MD) were cultured in L-15 medium which contained fetal calf serum (10%), penicillin (0.06 mg/ml), streptomycin (0.1 mg/ml), and Fungizone (0.01 mg/ml), buffered with L-arginine at pH 7.4 (reagents and medium from Invitrogen, Carlsbad, CA). Cells were grown at 37℃ in a 5% CO_2 atmosphere. In some studies, cells were treated with dynasore (80 μM, Sigma, St. Louis, MO) or the diluent, DMSO, for 1 hour and then prepared for microscopic image analysis. For time-lapse imaging the cells were maintained in the dynasore or diluent for the entire viewing time except in the recovery studies in which dynasore was washed out after an hour. In recovery studies, the cells were viewed for 30 minutes before adding the dynasore and for 2 hours after dynasore was washed out.

Gap junction antibodies and probes

Affinity purified polyclonal rabbit antibodies (IgG), prepared against synthetic peptides corresponding to the C-terminus of the Cx43 molecule (residues 370 to 381) (Yeager and Gilula, 1992) (Zymed Laboratory, San Francisco, CA). Preparation and characterization of these antibodies have been previously described (Kumar and Gilula, 1992). Monoclonal dynamin antibody was purchased from BD Transduction Laboratories™ (Rockville, MD) and clathrin antibody from Abcam (Cambridge, MA).

Immunocytochemistry

Cells were prepared and stained for connexin 43 and dynamin with immunocytochemical techniques, as previously described (Oyoyo et al., 1997). Prior to immunocytochemical procedures, the cells were grown on coverslips, rinsed with phosphate buffered saline solution (PBS), fixed at room temperature, in 3% formaldehyde for 20 minutes, permeabilized in cold acetone for 7 minutes, and then incubated at 37℃ for 1 hour or at 4℃ overnight in the connexin antibody. In some experiments following the connexin labeling, the cells were incubated at 4℃ overnight in the dynamin antibodies or clathrin antibody. The cells were then washed three times in PBS and incubated in Alexa Fluor 594 or 488 secondary antibodies (Invitrogen, Carlsbad, CA), diluted 1:1000 in PBS. The coverslips were stained with Hoescht, washed in PBS, and placed onto glass slides with a drop of Fluoromount-G anti-quench reagent (Southern Biotechnical Lab, Birmingham, AL). Immunolabeled cells were imaged at 63× with an Olympus Provis microscope (Olympus, Center Valley, PA). The 3D reconstruction images were captured on A1 Nikon Microscope and rendered with Elements Imaging Software (Nikon Instruments Inc., Melville, NY).

For immunocytochemical analysis, the size of gap junction plaques (length expressed as μm ± s.e.m.), annular gap junction vesicles (area expressed as μm^2 ± s.e.m.) and gap junction buds (area expressed as μm^2 ± s.e.m.) were determined by computer-assisted analysis with the MetaMorph software in control and treated cell cultures. The number of gap junction plaques and annular vesicles per cell nuclei were calculated. Annular gap junction vesicle size was measured from immunocytochemical images taken of dynasore, diluent-treated, and siRNA dynamin knockdown populations. Fluorescent spherical puncta that were greater-or-equal to 0.4 μm in diameter were classified as annular gap junction vesicles while plaques were identified by their typical elongated profile or by the presence of a puncta (smaller plaques), that were obviously at the cell surface between two cell pairs. The data are expressed as the average number of annular gap junction vesicles per cell.

The number of buds per plaque was obtained from counting 112 (taken from 4 samples) control and 110 (taken from 2 samples) dynamin knockdown plaques. The bud area was determined from 189 (collected from 157 different positions from 1 experiment) control and 55 (collected from 54 different positions from 1 experiment) dynasore bud measurements. The number of annular gap junctions per cell were measured from 124 (collected from 3 different positions from 1 experiment) control and 122 (collected from 2 different positions from 1 experiment) knockdown cells and from 386 (collected from 17 different positions from 3 experiments) DMSO control and 646 (collected from 34 different positions from 4 experiments) dynasore-treated cells. The number of cells was determined by counting the Hoechst stained nuclei in the samples. To determine the statistical significance of differences, the Student's *t*-test was used.

Percentage colocalization

The percentage colocalization was calculated from 50 cells (10 cells were selected from each of five files) confocal step through images were selected with elements at the mid-plane of the Z-stack) and saved as a tiff. The MetaMorph Software Program was used to view and trace the cell borders and to determine the percentage. Specifically, the merged image was separated into red and green channels and the trace areas were then transferred to the separated images. After thresholding the images, the number of Cx43-containing objects was determined with the automatic counting tool in MetaMorph. The counts were displayed on the 'record count screen', which was then analyzed and the number of surface gap junctions (as well as the number of clusters or aggregates or any object that did not look like an annular gap junction) were counted manually and subtracted from the total number of objects. The number of overlapping areas (yellow objects) were then counted manually by analyzing the merged image. The number of surface junctions that colocalized were determined by counting the number of surface gap junctions that had any yellow associated with them. The data are expressed as the average percentage colocalization of annular gap junction vesicles or surface gap junctions with dynamin.

Transfection with cDNA

To visualize gap junction trafficking in living cells, adrenal cells were transfected with cDNAs encoding the fluorescent Cx43-GFP (provided by Dr M. Falk, Lehigh University) and in addition in some experiments with CHC-mCherry (Dr Linton Traub, University of Pittsburgh). The Cx43-GFP vector was constructed by linking the GFP fluorescent reporter protein to the C-terminus of the rat Cx43 cDNA, and has been demonstrated to assemble into gap junction plaques similar to wild-type Cx43 (Falk, 2000). Lipofectamine 2000 Transfection Reagent (Invitrogen, Carlsbad, CA) was used to establish cell populations that transiently expressed fluorescently tagged Cx43, clathrin, empty vector, or GFP.

The day before transfection, cells were seeded onto coverslips or in MatTek cell culture dishes (MatTek Corporation, Ashland, MA). Cell populations, at 70–80% confluence, were transfected in optimem medium which contained Lipofectamine 2000 Transfection Reagent (Invitrogen, Carlsbad, CA) and 4 μg of plasmid DNA (Cx43-GFP, clathrin-mCherry, pCS2-RFP or empty vector) for 24 hours at 37℃ in an atmosphere of 5% CO_2. The resulting complexes were removed by gentle aspiration and washed with PBS. Fresh L-15 complete cell growth medium was added to the dishes, and the cells were incubated at 37℃ in 5% CO_2 for 24–48 hours before imaging. For dynamin knockdown, siRNA (Invitrogen, Carlsbad, CA) was transfected (20 nM) into the cells with Lipofectamine 2000 reagents.

Imaging of Cx43-GFP in living cells

Mattek glass bottom dishes with cells expressing Cx43-GFP, pCS2-RFP or CHC-mCherry were placed into a temperature controlled chamber and maintained at 37℃ in 5% CO_2 on a live cell IX-81 Olympus or a Nikon A1 series confocal laser point scanning system (Nikon Instruments Inc., Melville, NY). Image acquisition on the Olympus was performed with a MetaMorph Imaging System (Molecular Devices, Downington, PA) and Nikon Elements on the A1 Nikon microscope. The culture media was supplemented with 10 mM HEPES, pH 7.2 and, in some cases, DMSO or 80 μM dynasore was added to the chamber.

Images were obtained with a 63× oil objective and a numerical aperture of 1.4. Images were collected at 1–5-minute intervals with a fully-automated Nikon A1 laser scanning confocal microscope. DIC and fluorescent images were obtained using the standard fluorescence detector at wavelengths 482 and 595 for all experiments. Focus was maintained with the Perfect Focus System (PFS) function and images were acquired with Nikon's Elements software. The 3D images were captured such that the *xyz* dimensions were 0.5 μm^3. The data sets were analyzed both qualitatively and quantitatively, and were analyzed with the volume rendering tool in Elements. The time lapse images were converted to movies.

Time-lapse images were to used analyze gap junction plaque internalization in control and dynasore-treated cells. For analysis, time-lapse movies were evaluated with the MetaMorph program (Molecular Devices, Downington, PA).

Annular gap junction vesicle pattern of displacement within the cell and corresponding changes in size (area expressed as μm^2) were quantified with the tracking function in the Imaris analysis software (Bitplane Scientific, South Windsor, CT). Selected annular vesicles were segmented based upon labeling intensity and then followed over time. Annular gap junction fission was monitored both qualitatively and quantitatively by observing the split of the one vesicle (thresholded to appear yellow in the examples shown) into two vesicles (one thresholded to appear yellow and the other one red). Quantitatively fission was monitored by measuring and graphing annular gap junction size (area) over time. The times at which the fission occurred and the area of the vesicles were noted and compared. The number of fissions/hour were determined from 25 control and 19 dynasore imaging positions. Statistical significance of differences was determined with the Student's *t*-test.

Transmission electron microscopy

Cell monolayers were briefly rinsed in PBS then fixed with 2.5% glutaraldehyde in PBS, pH 7.4, for 1 hour at room temperature. All samples were then washed three times in PBS buffer and post-fixed for 1 hour at 4℃ in 1% osmium tetroxide with 1% potassium ferricyanide. For pre-embedding quantum dot immuno-staining for clathrin, cells were fixed in 2% paraformaldehyde and 0.1% glutaraldehyde in PBS as previously described (Ogunkoya et al., 2009). The samples were washed again and the cells were then serially dehydrated in a ethanol (30%, 50%, 70% and 90%) for 10 minutes and then for 15 minutes in 100% ethanol three times. The cells were then incubated in Epon three times for 1 hour and finally embedded in resin to be sectioned. Ultra-thin sections were cut, mounted on grids, and imaged on a JEOL 1011CX electron microscope (JEOL, Tokyo, Japan).

Transferrin uptake

To monitor the cell's capacity for internalization, the capacity for transferrin receptors uptake was analyzed. Transferrin receptors uptake was monitored by incubation in medium containing 10 μg/ml Alexa-Fluor-594-labeled transferrin (Invitrogen, Carlsbad, CA) for 15 minutes, at 37℃, followed by fixation and microscopic examination.

Acknowledgements

We acknowledge Dr Nalin Kumar's gift of antibodies, Drs Linton Traub and Matthias Falk's contribution of plasmids, and the technical support of Kevin Alber, Ming Sun and Shakira O'Neil at the University of Pittsburgh.

Author contributions

S.A.M. designed and performed experiments, interpreted data, and wrote the manuscript, B.M.N. designed and performed experiments, interpreted data, and wrote the manuscript and M.B, K.S. and T.I.S. performed experiments, interpreted data, and edited the manuscript, and V.G. interpreted data, and edited the manuscript.

Funding

This work was supported by grants from the National Science Foundation (NSF) [grant number MCB-1023144] and National Institutes of Health (NIH) [grant number H-5T36GM008622]. Deposited in PMC for release after 12 months.

Supplementary material available online at
http://jcs.biologists.org/lookup/suppl/doi:10.1242/jcs.116269/-/DC1

References

Ahmad, S., Diez, J. A., George, C. H. and Evans, W. H. (1999). Synthesis and assembly of connexins in vitro into homomeric and heteromeric functional gap junction hemichannels. *Biochem. J.* **339**, 247-253.

Bachran, D., Schneider, S., Bachran, C., Weng, A., Melzig, M. F. and Fuchs, H. (2011). The endocytic uptake pathways of targeted toxins are influenced by synergistically acting Gypsophila saponins. *Mol. Pharm.* **8**, 2262-2272.

Bejarano, E., Girao, H., Yuste, A., Patel, B., Marques, C., Spray, D. C., Pereira, P. and Cuervo, A. M. (2012). Autophagy modulates dynamics of connexins at the plasma membrane in a ubiquitin-dependent manner. *Mol. Biol. Cell* **23**, 2156-2169.

Chanson, M., Derouette, J. P., Roth, I., Foglia, B., Scerri, I., Dudez, T. and Kwak, B. R. (2005). Gap junctional communication in tissue inflammation and repair. *Biochim. Biophys. Acta* **1711**, 197-207.

De Camilli, P., Takei, K. and McPherson, P. S. (1995). The function of dynamin in endocytosis. *Curr. Opin. Neurobiol.* **5**, 559-565.

Defranco, B. H., Nickel, B. M., Baty, C. J., Martinez, J. S., Gay, V. L., Sandulache, V. C., Hackam, D. J. and Murray, S. A. (2008). Migrating cells retain gap junction plaque structure and function. *Cell Commun. Adhes.* **15**, 273-288.

Elgass, K., Pakay, J., Ryan, M. T. and Palmer, C. S. (2013). Recent advances into the understanding of mitochondrial fission. *Biochim. Biophys. Acta* **1833**, 150-161.

Evans, W. H. and Martin, P. E. (2002). Lighting up gap junction channels in a flash. *Bioessays* **24**, 876-880.

Falk, M. M. (2000). Connexin-specific distribution within gap junctions revealed in living cells. *J. Cell Sci.* **113**, 4109-4120.

Fessart, D., Simaan, M. and Laporte, S. A. (2005). c-Src regulates clathrin adapter protein 2 interaction with beta-arrestin and the angiotensin II type 1 receptor during clathrin- mediated internalization. *Mol. Endocrinol.* **19**, 491-503.

Fiorini, C., Gilleron, J., Carette, D., Valette, A., Tilloy, A., Chevalier, S., Segretain, D. and Pointis, G. (2008). Accelerated internalization of junctional membrane proteins (connexin 43, N-cadherin and ZO-1) within endocytic vacuoles: an early event of DDT carcinogenicity. *Biochim. Biophys. Acta* **1778**, 56-67.

Fong, J. T., Kells, R. M., Gumpert, A. M., Marzillier, J. Y., Davidson, M. W. and Falk, M. M. (2012). Internalized gap junctions are degraded by autophagy. *Autophagy* **8**, 794-811.

Gilleron, J., Carette, D., Fiorini, C., Dompierre, J., Macia, E., Denizot, J. P., Segretain, D. and Pointis, G. (2011). The large GTPase dynamin2: a new player in

connexin 43 gap junction endocytosis, recycling and degradation. *Int. J. Biochem. Cell Biol.* **43**, 1208-1217.

Goodenough, D. A., Goliger, J. A. and Paul, D. L. (1996). Connexins, connexons, and intercellular communication. (Review). *Annu. Rev. Biochem.* **65**, 475-502.

Gumpert, A. M., Varco, J. S., Baker, S. M., Piehl, M. and Falk, M. M. (2008). Double-membrane gap junction internalization requires the clathrin-mediated endocytic machinery. *FEBS Lett.* **582**, 2887-2892.

Hill, E., van Der Kaay, J., Downes, C. P. and Smythe, E. (2001). The role of dynamin and its binding partners in coated pit invagination and scission. *J. Cell Biol.* **152**, 309-323.

Hoppins, S., Lackner, L. and Nunnari, J. (2007). The machines that divide and fuse mitochondria. *Annu. Rev. Biochem.* **76**, 751-780.

Iversen, T. G., Skretting, G., van Deurs, B. and Sandvig, K. (2003). Clathrin-coated pits with long, dynamin-wrapped necks upon expression of a clathrin antisense RNA. *Proc. Natl. Acad. Sci. USA* **100**, 5175-5180.

Jordan, K., Solan, J. L., Dominguez, M., Sia, M., Hand, A., Lampe, P. D. and Laird, D. W. (1999). Trafficking, assembly, and function of a connexin43-green fluorescent protein chimera in live mammalian cells. *Mol. Biol. Cell* **10**, 2033-2050.

Jordan, K., Chodock, R., Hand, A. R. and Laird, D. W. (2001). The origin of annular junctions: a mechanism of gap junction internalization. *J. Cell Sci.* **114**, 763-773.

Kirchhausen, T. (2000a). Clathrin. *Annu. Rev. Biochem.* **69**, 699-727.

Kirchhausen, T. (2000b). Three ways to make a vesicle. *Nat. Rev. Mol. Cell Biol.* **1**, 187-198.

Kirchhausen, T., Macia, E. and Pelish, H. E. (2008). Use of dynasore, the small molecule inhibitor of dynamin, in the regulation of endocytosis. *Methods Enzymol.* **438**, 77-93.

Kirkham, M. and Parton, R. G. (2005). Clathrin-independent endocytosis: new insights into caveolae and non-caveolar lipid raft carriers. *Biochim. Biophys. Acta* **1746**, 349-363.

Kumar, N. M. and Gilula, N. B. (1992). Molecular biology and genetics of gap junction channels. *Semin. Cell Biol.* **3**, 3-16.

Larsen, W. J. and HAI-NAN, (1978). Origin and fate of cytoplasmic gap junctional vesicles in rabbit granulosa cells. *Tissue Cell* **10**, 585-598.

Larsen, W. J., Tung, H. N., Murray, S. A. and Swenson, C. A. (1979). Evidence for the participation of actin microfilaments and bristle coats in the internalization of gap junction membrane. *J. Cell Biol.* **83**, 576-587.

Lauf, U., Giepmans, B. N., Lopez, P., Braconnot, S., Chen, S. C. and Falk, M. M. (2002). Dynamic trafficking and delivery of connexons to the plasma membrane and accretion to gap junctions in living cells. *Proc. Natl. Acad. Sci. USA* **99**, 10446-10451.

Leithe, E., Brech, A. and Rivedal, E. (2006a). Endocytic processing of connexin43 gap junctions: a morphological study. *Biochem. J.* **393**, 59-67.

Leithe, E., Sirnes, S., Omori, Y. and Rivedal, E. (2006b). Downregulation of gap junctions in cancer cells. *Crit. Rev. Oncog.* **12**, 225-256.

Lichtenstein, A., Minogue, P. J., Beyer, E. C. and Berthoud, V. M. (2011). Autophagy: a pathway that contributes to connexin degradation. *J. Cell Sci.* **124**, 910-920.

Macia, E., Ehrlich, M., Massol, R., Boucrot, E., Brunner, C. and Kirchhausen, T. (2006). Dynasore, a cell-permeable inhibitor of dynamin. *Dev. Cell* **10**, 839-850.

Murray, S. A., Larsen, W. J., Trout, J. and Donta, S. T. (1981). Gap junction assembly and endocytosis correlated with patterns of growth in a cultured adrenocortical tumor cell (SW-13). *Cancer Res.* **41**, 4063-4074.

Murray, S. A., Williams, S. Y., Dillard, C. Y., Narayanan, S. K. and McCauley, J. (1997). Relationship of cytoskeletal filaments to annular gap junction expression in human adrenal cortical tumor cells in culture. *Exp. Cell Res.* **234**, 398-404.

Nankoe, S. R. and Sever, S. (2006). Dynasore puts a new spin on dynamin: a surprising dual role during vesicle formation. *Trends Cell Biol.* **16**, 607-609.

Nickel, B. M., DeFranco, B. H., Gay, V. L. and Murray, S. A. (2008). Clathrin and Cx43 gap junction plaque endoexocytosis. *Biochem. Biophys. Res. Commun.* **374**, 679-682.

Ogunkoya, Y., Nickel, B. M., Gay, V. L. and Murray, S. A. (2009). Using quantum dots to visualize clathrin associations. *Biotech. Histochem.* **84**, 109-115.

Oyoyo, U. A., Shah, U. S. and Murray, S. A. (1997). The role of alpha1 (connexin-43) gap junction expression in adrenal cortical cell function. *Endocrinology* **138**, 5385-5397.

Pahujaa, M., Anikin, M. and Goldberg, G. S. (2007). Phosphorylation of connexin43 induced by Src: regulation of gap junctional communication between transformed cells. *Exp. Cell Res.* **313**, 4083-4090.

Piehl, M., Lehmann, C., Gumpert, A., Denizot, J. P., Segretain, D. and Falk, M. M. (2007). Internalization of large double-membrane intercellular vesicles by a clathrin-dependent endocytic process. *Mol. Biol. Cell* **18**, 337-347.

Rappoport, J. Z., Heyman, K. P., Kemal, S. and Simon, S. M. (2008). Dynamics of dynamin during clathrin mediated endocytosis in PC12 cells. *PLoS ONE* **3**, e2416.

Robinson, M. S. (1994). The role of clathrin, adaptors and dynamin in endocytosis. *Curr. Opin. Cell Biol.* **6**, 538-544.

Roux, A. and Antonny, B. (2008). The long and short of membrane fission. *Cell* **135**, 1163-1165.

Scott, I. and Youle, R. J. (2010). Mitochondrial fission and fusion. *Essays Biochem.* **47**, 85-98.

Segretain, D. and Falk, M. M. (2004). Regulation of connexin biosynthesis, assembly, gap junction formation, and removal. *Biochim. Biophys. Acta* **1662**, 3-21.

Sigismund, S., Woelk, T., Puri, C., Maspero, E., Tacchetti, C., Transidico, P., Di Fiore, P. P. and Polo, S. (2005). Clathrin-independent endocytosis of ubiquitinated cargos. *Proc. Natl. Acad. Sci. USA* **102**, 2760-2765.

Smirnova, E., Griparic, L., Shurland, D. L. and van der Bliek, A. M. (2001). Dynamin-related protein Drp1 is required for mitochondrial division in mammalian cells. *Mol. Biol. Cell* **12**, 2245-2256.

Solan, J. L. and Lampe, P. D. (2005). Connexin phosphorylation as a regulatory event linked to gap junction channel assembly. *Biochim. Biophys. Acta* **1711**, 154-163.

Solan, J. L. and Lampe, P. D. (2009). Connexin43 phosphorylation: structural changes and biological effects. *Biochem. J.* **419**, 261-272.

Sosinsky, G. E., Gaietta, G. M., Hand, G., Deerinck, T. J., Han, A., Mackey, M., Adams, S. R., Bouwer, J., Tsien, R. Y. and Ellisman, M. H. (2003). Tetracysteine genetic tags complexed with biarsenical ligands as a tool for investigating gap junction structure and dynamics. *Cell Commun. Adhes.* **10**, 181-186.

Strack, S. and Cribbs, J. T. (2012). Allosteric modulation of Drp1 mechanoenzyme assembly and mitochondrial fission by the variable domain. *J. Biol. Chem.* **287**, 10990-11001.

Ungewickell, E. J. and Hinrichsen, L. (2007). Endocytosis: clathrin-mediated membrane budding. *Curr. Opin. Cell Biol.* **19**, 417-425.

Yeager, M. and Gilula, N. B. (1992). Membrane topology and quaternary structure of cardiac gap junction ion channels. *J. Mol. Biol.* **223**, 929-948.

Young, A., Gentzsch, M., Abban, C. Y., Jia, Y., Meneses, P. I., Bridges, R. J. and Bradbury, N. A. (2009). Dynasore inhibits removal of wild-type and DeltaF508 cystic fibrosis transmembrane conductance regulator (CFTR) from the plasma membrane. *Biochem. J.* **421**, 377-385.

Movie 1. Time-lapse movie of gap junction plaque endoexocytosis seen in Fig. 4B. The invagination of the gap junction plaque (Cx43-GFP) is seen over time to result in the release of an annular gap junction. The two adjacent cells are expressing Cx43-GFP; however, only one is expressing clathrin-mCherry (which helps to define the boundaries of that cell). The annular gap junction is released into a cell that is not expressing the clathrin-mCherry. During the 10-hour viewing period, images were collected every 2 minutes.

Movie 2. Time-lapse movie of gap junction plaque endoexocytosis in the DMSO control population, seen in Fig. 5A. Images were collected every 2 minutes.

Movie 3. **Time-lapse movie of gap junction plaque endoexocytosis in the dynasore treated population, seen in Fig. 5B.** Images were collected every 2 minutes.

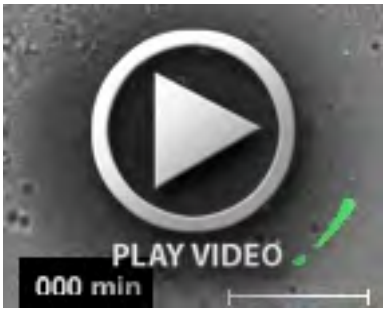

Movie 4. Time-lapse movie demonstrating the recovery from dynasore inhibition of internalization, seen in Fig. 6. Images were collected every 1 minute. There was a shift in the position of the stage at the point that dynasore was added (*t*=30 minutes). Dynasore was washed out and new growth media was added at *t*=90 minutes).

Movie 5. Time-lapse imaging and tracking of annular gap junction vesicle fission in the DMSO control cell, seen in Fig. 7H. Images were collected every 1 minute.

Movie 6. Time-lapse imaging and tracking of annular gap junction vesicle fission in the dynasore treated cell, seen in Fig. 7I. Images were collected every 1 minute.